COBEM 2021 26th International Congress of Mechanical Engineering
ABCM Associação Brasileira de Engenharia e Ciências Mecânicas
November 22-26, 2021, Virtual Congress, Brazil

COB-2021-0434
TIME DOMAIN IDENTIFICATION OF DYNAMIC PARAMETERS OF MAGNETIC BEARINGS USING STATISTICAL LEARNING METHODS

Felipe Lourenço Angelim Vieira
Diego Alejandro Godoy Diaz
Fernando Augusto de Noronha Castro Pinto
Universidade Federal do Rio de Janeiro, Department of Mechanical Engineering, Cidade Universitária - Ilha do Fundão, CEP 21945-970, Rio de Janeiro, RJ - Brazil
felipeangelim@gmail.com
dgodoy@ufrj.br
fcpinto@ufrj.br

Abstract. *Magnetic bearings are used to control and monitor rotating machinery, and modelling its behavior is essential for understanding the limitations of the system in operation. However, the experimental conditions for identification of their parameters cannot be maintained for long. The noise in observations is usually bypassed by the use of methods in frequency domain and the acquisition of data during multiple periods. In this work, we propose the use of Savitzky-Golay filter for noise attenuation and two methods for time domain identification of dynamic coefficients. The first is based on optimization algorithms adopted by machine learning literature. The second one is a linear regression that favors online estimation of parameters. Both methods demonstrated similar results when compared to a baseline frequency-domain method, when the system is excited by harmonic signals. The use of linear regression with multisine excitation was also analyzed.*

Keywords: *magnetic bearings, system identification, dynamic stiffness, Savitzky-Golay, simple linear regression*

1. INTRODUCTION

Active Magnetic Bearings (AMB) are free of contact bearings used to suspend a spinning rotor at high rotating speeds. They use the magnetic field created by moving electric charges to apply attractive forces to the rotor, requiring position sensors and a closed-loop control to continuously adapt the field intensity. The applications of AMBs include synchronous vibration suppression in flexible rotors (Das and Dutt (2010)), detection of bearing faults (Chasalevris *et al.* (2014)) and of cracked rotors (Zhu *et al.* (2003)), and identification of dynamic parameters of annular seals (Diaz (2016)).

Determining the dynamic behaviour of magnetic bearings is needed when we are interested in detecting faults and understanding stability limitations of the system. Frequency-domain methods are the most common approach to identify the dynamic parameters of bearings (Tiwari *et al.* (2004)). In such approach, the system is excited with a suitable signal and the spectrum of inputs and outputs are used to infer the parameters of the system. This usually involves acquiring the results during multiple periods to increase the signal-to-noise ratio.

A time-domain approach, on the other hand, may introduce prior knowledge about the expected measurements, such as smoothness or signal shape, to attenuate the noise. The data volume also favors the use of methods adopted by machine learning literature, such as gradient-based optimization algorithms. The gradient-based optimization algorithms are well-known for their applications in neural networks and obtained special attention in machine learning literature after Krizhevsky *et al.* (2012). Neural network based methods are state-of-the-art in classification and generation of image and audio (Karras *et al.*, 2019; Donahue and Simonyan, 2019; Karras *et al.*, 2020; Dhariwal *et al.*, 2020), in natural language processing (Brown *et al.*, 2020; Devlin *et al.*, 2018; Vaswani *et al.*, 2017) and reinforcement learning (Lillicrap *et al.*, 2015; Mnih *et al.*, 2013; Robbins and Monro, 1951; Schulman *et al.*, 2017; Zou *et al.*, 2019). Recently, gradient-based optimization was used to estimate the Lagrangian and Hamiltonian of physical systems (Cranmer *et al.*, 2020; Greydanus *et al.*, 2019).

In this work, we propose a time-domain approach which favors online estimation of dynamic parameters of magnetic bearings. First, noise reduction is achieved by applying the Savitzky-Golay filter to position and force data, when the system is excited with harmonic signals. Then, two methods are proposed to determine the dynamic coefficients: an ordinary linear regression (OLS) and gradient descent optimization. An approach for multisine excitation signals is also proposed.

2. AMB System Model

In this section, the hypothesis and modelling of the system will be explained. First, the modelling of the rotor is detailed. Then, we add the forces of the magnetic bearing controlled by a PID scheme to the motion equations of the rotor.

Consider a uniform, rigid and balanced rotor, modelled as a single element of mass m, width l and diameter d. To describe the body dynamics, we define four coordinates systems built from successive rotations: R (r_x, r_y, r_z) is the inertial coordinate system, the other three systems A (a_x, a_y, a_z), B (b_x, b_y, b_z), C (c_x, c_y, c_z) are defined from successive rotations along θr_x, βa_y and Ωb_z, respectively. These angles are also known as Cardan angles. The inertia matrix $\mathbf{I}^{C/C^*}$ is symmetric and diagonal, as defined in Eq. (1):

$$\mathbf{I}^{C/C^*} = \begin{bmatrix} I_x & 0 & 0 \\ 0 & I_y & 0 \\ 0 & 0 & I_z \end{bmatrix}, \qquad I_x = I_y = \frac{1}{16}md^2 + \frac{1}{12}ml^2,\ I_z = \frac{1}{8}md^2 \tag{1}$$

where C denotes the rotor and C^* its center of mass. In the case of a balanced rotor, the mass matrix $\mathbf{M}$ is diagonal:

$$\mathbf{M} = \begin{bmatrix} m & 0 & 0 \\ 0 & m & 0 \\ 0 & 0 & m \end{bmatrix} \tag{2}$$

The Newton-Euler equations in Eq. (3) describe the dynamics of the body:

$$\begin{bmatrix} F_{ext} \\ M_{ext}^{C/C^*} \end{bmatrix} = \begin{bmatrix} \mathbf{M} & 0 \\ 0 & \mathbf{I}^{C/C^*} \end{bmatrix} \begin{bmatrix} {}^{R}a^{C} \\ {}^{R}\dot{\omega}^{S} \end{bmatrix} + \begin{bmatrix} 0 \\ {}^{R}\omega^{S} \times (\mathbf{I}^{C/C^*}\,{}^{R}\omega^{S}) \end{bmatrix} \tag{3}$$

where $F_{ext} \in \mathbb{R}^3$ and $M_{ext}^{C/C^*} \in \mathbb{R}^3$ are, respectively, the vector of external forces and external moments , $\mathbf{M} \in \mathbb{R}^{3\times3}$ is the mass matrix, ${}^{R}a^{C} = \begin{bmatrix} \ddot{x} & \ddot{y} & \ddot{z} \end{bmatrix}^T$ is the accelaration of the body and ${}^{R}\omega^{S} = \begin{bmatrix} \dot{\theta} & \dot{\beta} & \dot{\Omega} \end{bmatrix}^T$ its angular velocity. Considering that rotations along radial directions are sufficiently small, we can linearize Eq. (3) and express the dynamics of the body with respect to generalized coordinates $q = \begin{bmatrix} x(t) & \theta(t) & y(t) & \beta(t) \end{bmatrix}^T$:

$$\mathbf{M}\ddot{q} + \dot{\Omega}\mathbf{G}\dot{q} = F_{ext} \tag{4}$$

$$\mathbf{M} = \begin{bmatrix} m & 0 & 0 & 0 \\ 0 & I_x & 0 & 0 \\ 0 & 0 & m & 0 \\ 0 & 0 & 0 & I_y \end{bmatrix}, \mathbf{G} = \begin{bmatrix} 0 & 0 & 0 & 0 \\ 0 & 0 & 0 & I_z \\ 0 & 0 & 0 & 0 \\ 0 & -I_z & 0 & 0 \end{bmatrix}$$

In this work, the rotor is submitted to equal external forces at both ends and Eq. (4) can be further simplified:

$$\mathbf{M}\ddot{p} = F_{ext} = F_g + F_{bearing} + F_{exc} \tag{5}$$

$$\mathbf{M} = \begin{bmatrix} m & 0 \\ 0 & m \end{bmatrix}$$

where $\ddot{p} = \begin{bmatrix} \ddot{x}(t) & \ddot{y}(t) \end{bmatrix}^T$ is acceleration vector, F_g is the gravitational force, $F_{bearing}$ is the force applied by the AMB to stabilise the rotor and F_{exc} is the excitation force applied to the system. The bearing forces are characterized by its stiffness and damping matrices (Schweitzer and Maslen (2009)), which depend on the choosen closed-loop control method and excitation frequency. Including those components in Eq. (5) we obtain:

$$\mathbf{M}\ddot{p} + \mathbf{K}p + \mathbf{C}\dot{p} = F_{ext} = F_g + F_{exc} \tag{6}$$

where $\mathbf{K}$ is stiffness matrix and $\mathbf{C}$ is damping matrix. The estimators explained in the following sections aim at determining these matrices for different frequencies.

3. TIME-DOMAIN ESTIMATION

In this section, the proposed methods for time-domain estimation of stiffness and damping matrices are presented. First, we describe how the coefficients can be estimated with optimization algorithms and ordinary linear regression by using the data of harmonic excitation. Then, we explain how we can remove the noise of the signal with Savitzky-Golay filter. This filter also provides estimates of the velocity and rotor acceleration, which are needed for time-domain methods. Finally, we detail how these methods can be applied to data acquired with multisine excitation signal.

3.1 ESTIMATION WITH GRADIENT DESCENT

The estimation of stiffness and damping matrices can be written as an optimization problem. An estimator of acceleration of can be derived from Eq. (6):

$$\ddot{q} = f_\theta(F_{exc}, \dot{q}, q) = \mathbf{M}^{-1}(F_{exc} + F_g - \mathbf{C}_{\theta_1}\dot{q} - \mathbf{K}_{\theta_2}q), \quad \theta = \{\theta_1, \theta_2\} \tag{7}$$

where θ_1 and θ_2 are the damping and stiffness coefficients.

Given a differentiable error metric $\mathcal{L}$, we can back-propagate the errors of predicted acceleration to approximate the matrices to their true values. The optimization problem is stated in Eq. (8).

$$\min_\theta \ \mathcal{L}(f_\theta(F_{exc}, \dot{q}, q), \ddot{q}) \tag{8}$$

In this work, mean squared error was chosen as error metric and Adam (Kingma and Ba, 2014) was used as optimization method.

3.2 ESTIMATION WITH ORDINARY LINEAR REGRESSION

The dynamics of the rotor can be written in the form of classic linear regression problem, where damping and stiffness are the unknown coefficients. The following equation:

$$\mathbf{C}_{\theta_1}\dot{p}(t) + \mathbf{K}_{\theta_2}p(t) = F_{exc}(t) + F_g - \mathbf{M}\ddot{p}(t) = f^*(t) \tag{9}$$

$$\mathbf{C}_{\theta_1} = \begin{bmatrix} C_{xx} & C_{yy} \\ C_{yx} & C_{yy} \end{bmatrix}, \quad \mathbf{K}_{\theta_2} = \begin{bmatrix} K_{xx} & K_{yy} \\ K_{yx} & K_{yy} \end{bmatrix}$$

,

is equivalent to Eq. (10), provided a dataset of N observations:

$$\begin{bmatrix} \dot{x}(t_1) & \dot{y}(t_1) & x(t_1) & y(t_1) \\ \vdots & \vdots & \vdots & \vdots \\ \dot{x}(t_N) & \dot{y}(t_N) & x(t_N) & y(t_N) \end{bmatrix} \begin{bmatrix} C_{xx} & C_{yx} \\ C_{xy} & C_{yy} \\ K_{xx} & K_{yx} \\ K_{xy} & K_{yy} \end{bmatrix} = \begin{bmatrix} f_x^*(t_1) & f_y^*(t_1) \\ \vdots & \vdots \\ f_x^*(t_N) & f_y^*(t_N) \end{bmatrix} \tag{10}$$

where $x(t)$ and $y(t)$ are measured positions of the rotor center of mass along r_x and r_y at time t, and f_x^* and f_y^* are components of $f^*(t)$ along r_x and r_y. The solution that minimizes the mean squared error is (Hastie *et al.*, 2009):

$$\hat{\beta} = (X^T X)^{-1} X^T Y \tag{11}$$

where

$$X = \begin{bmatrix} \dot{x}(t_1) & \dot{y}(t_1) & x(t_1) & y(t_1) \\ \vdots & \vdots & \vdots & \vdots \\ \dot{x}(t_N) & \dot{y}(t_N) & x(t_N) & y(t_N) \end{bmatrix}, \quad \beta = \begin{bmatrix} C_{xx} & C_{yx} \\ C_{xy} & C_{yy} \\ K_{xx} & K_{yx} \\ K_{xy} & K_{yy} \end{bmatrix} \quad Y = \begin{bmatrix} f_x^*(t_1) & f_y^*(t_1) \\ \vdots & \vdots \\ f_x^*(t_N) & f_y^*(t_N) \end{bmatrix}$$

and $\hat{\beta}$ represents the β inferred by the regression.

3.3 SAVITZKY-GOLAY FILTERING AND DIFFERENTIATION

Both the gradient-based method and the linear regression require derivatives of measured position. Linear regression also needs explanatory variables with high signal-to-noise ratio in order to be consistent. Savitzky-Golay smoothing fits polynomials to moving windows and provides estimates of derivatives by differentiating the fitted polynomials (Savitzky and Golay, 1964). The filter coefficients depend on three parameters: the degree of the polynomial n, the window width m and differentiation order d (Gorry, 1990). Higher degrees and lower window widths provide filters with higher cut-off frequency.

3.4 ESTIMATION WITH MULTISINE EXCITATIONS

Both gradient-based method and linear regression can be adapted to estimate the bearing's coefficients with multisine excitation. Regarding multisine excitation, the contribution of each frequency to the observed position and force can be estimated. This is achieved by using a Savitzky-Golay filter with sines and cosines as basis functions, instead of polynomials. Regressing orthogonal harmonic series to the data provides the amplitudes and phases of each sub-series that compose the multisine signal. In other words, we project the measured multisine position series onto orthogonal harmonic series, which are noiseless. Then, time-domain methods can be applied in the same manner they are when the system is excited with harmonic signals.

Due to trigonometric identity, the multisine equation can be rewritten as:

$$u(t) = \sum_{k=1}^{N_f} u_k = \sum_{k=1}^{N_f} [A_{1_k} \sin(2\pi f_k t) + A_{2_k} \cos(2\pi f_k t)] \tag{12}$$

which is equivalent to:

$$\Phi A = U \tag{13}$$

where

$$\Phi = \begin{bmatrix} \sin(2\pi f_1 t_1) & \cos(2\pi f_1 t_1) & \dots & \sin(2\pi f_{N_f} t_1) & \cos(2\pi f_{N_f} t_1) \\ \sin(2\pi f_1 t_2) & \cos(2\pi f_1 t_2) & \dots & \sin(2\pi f_{N_f} t_2) & \cos(2\pi f_{N_f} t_2) \\ \vdots & \vdots & & \vdots & \vdots \\ \sin(2\pi f_1 t_{N-1}) & \cos(2\pi f_1 t_{N-1}) & \dots & \sin(2\pi f_{N_f} t_{N-1}) & \cos(2\pi f_{N_f} t_{N-1}) \\ \sin(2\pi f_1 t_N) & \cos(2\pi f_1 t_N) & \dots & \sin(2\pi f_{N_f} t_N) & \cos(2\pi f_{N_f} t_N) \end{bmatrix}, \quad A = \begin{bmatrix} A_{1_1} \\ A_{2_1} \\ \vdots \\ A_{1_{N_f}} \\ A_{2_{N_f}} \end{bmatrix}, \quad U = \begin{bmatrix} u(t_1) \\ u(t_2) \\ \vdots \\ u(t_{N-1}) \\ u(t_N) \end{bmatrix}$$

A regression can be used to find the coefficients A:

$$\hat{A} = (\Phi^T \Phi)^{-1} \Phi^T U \tag{14}$$

Fitting this regression to the force and measured position, we can obtain the position and corresponding force time-series of the selected set of frequencies. The velocity and acceleration can be found by differentiating the sine and cossine terms with respect to t:

$$\hat{u}_k(t) = \hat{A}_{1_k} \sin(2\pi f_k t) + \hat{A}_{2_k} \cos(2\pi f_k t) \tag{15}$$

$$\hat{\dot{u}}_k(t) = \hat{A}_{1_k} 2\pi f_k \cos(2\pi f_k t) - \hat{A}_{2_k} 2\pi f_k \sin(2\pi f_k t) \tag{16}$$

$$\hat{\ddot{u}}_k(t) = -\hat{A}_{1_k} (2\pi f_k)^2 \sin(2\pi f_k t) - \hat{A}_{2_k} (2\pi f_k)^2 \cos(2\pi f_k t) \tag{17}$$

With position, velocity and force components for each frequency f_k, $k \in \{1, \dots, N_f\}$, the stiffness and damping coefficients are obtained in the same manner as harmonic excitations.

4. EXPERIMENTAL SETUP

The experimental setup (illustrated in Fig. 1) is composed of two position sensors arranged near the ends of a small rotor, whose levitation is achieved by two heteropolar magnetic bearings systems (Siqueira (2013)). The system is submitted to excitation signals ranging from 5 Hz to 69 Hz and a PID controller allows the hovering of the the rotor around the center of the bearings. The AMB bearing parameters are listed in Table 1.

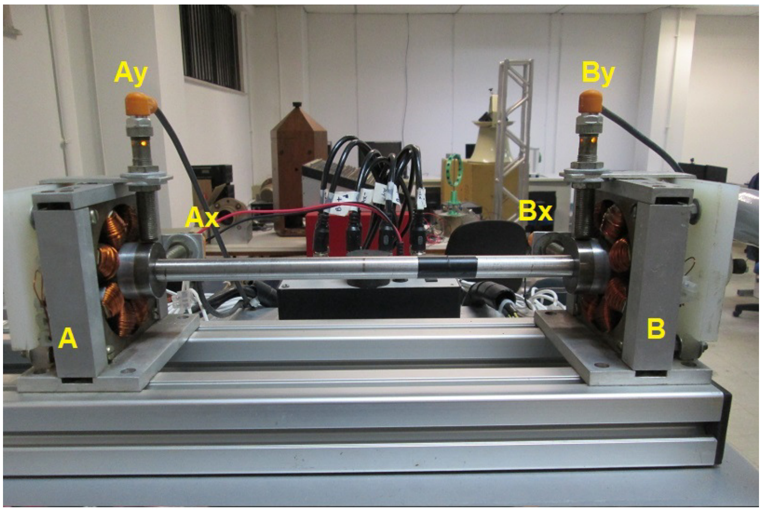

Figure 1: The experimental bench consists of a rotor with two ends A and B. The horizontal displacement is measured by two position sensors Ax and Bx, while the vertical position is measured by sensors Ay and By.

The data acquired from the experimental bench consists of position data of the rotor at A and B, and the magnitude of excitation signal sent to the bearings. The sample rate was 5.12 kHz. The force applied by the AMB due to the excitation signal can be computed from the measured electrical current and the rotor displacement (Diaz (2016)). Figure 2 shows position and force data of the system excited by harmonic signal of 5 Hz.

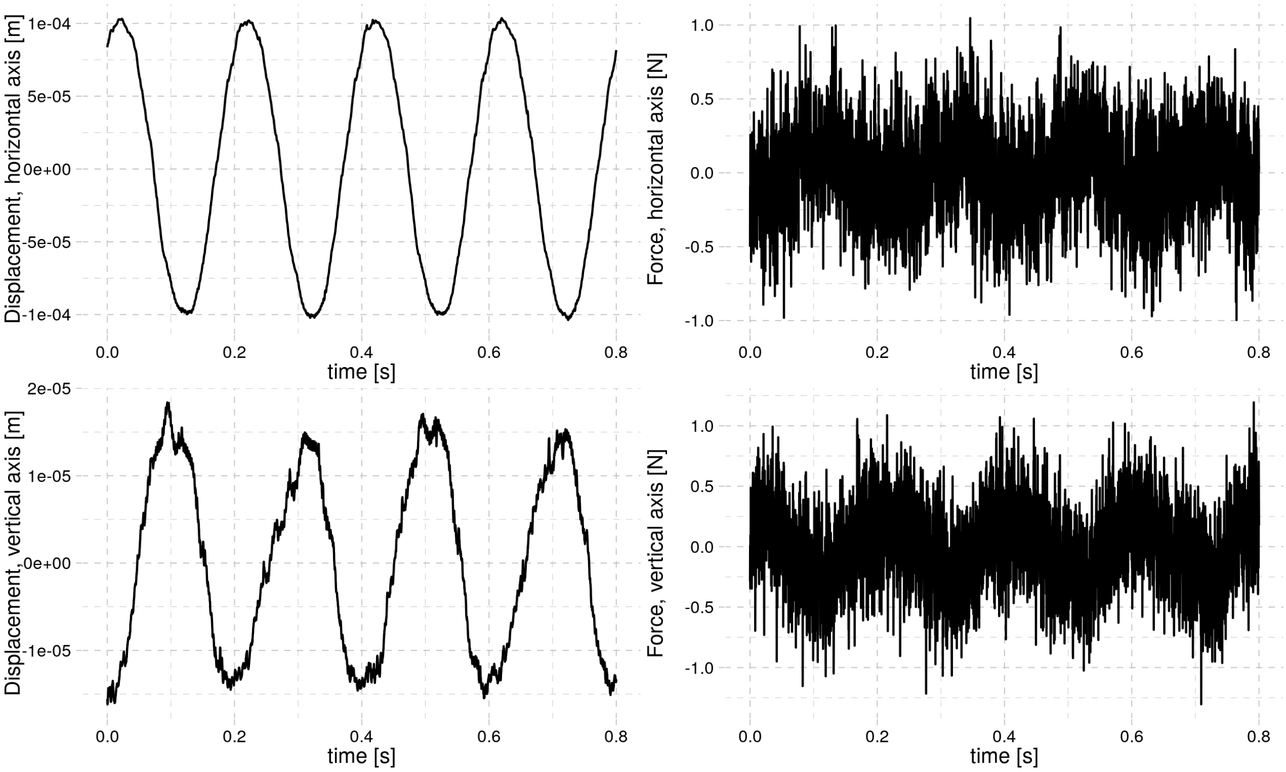

Figure 2: Bearing submitted to harmonic signal of 5 Hz. The position measures (m) are shown on the left and the forces (N) on the right.

Table 1: AMB parameters (Siqueira, 2013)

Parameter		Value	Unit.
Rotor‘s mass	m	1	kg
Rotor width	L_s	400	mm
Rotor diameter	d_s	14,28	mm
Bearing-rotor diameter	d_j	36,4	mm
Distance between actuators	$2a$	315	mm
Distance between sensors	$2b$	315	mm
Number of turns	N_v	130	Nm^{-1}
Base current	i_b	1	A
Air gap length	g_0	1	mm
Cross-sectional area of the pole	A_g	235	mm^2
Open loop stiffness	$K_{mag,x}$	-2,11e4	Nm^{-1}

4.1 EXCITATION SIGNALS

The choice of an excitation signal defines the experiment duration and it cannot expose the components to critic conditions. In general, we are interested in signals that allow a maximum of accuracy for given a peak value and experiment duration, due to practical conditions. The crest and time factors are two well-known measures to define the quality of a signal (Pintelon and Schoukens (2012)). The former represents the ratio of peak value and effective RMS value, and the latter characterizes how the power is allocated in the frequencies of interest. The lower these factors are, the better the estimations we can obtain in the time available for experiment.

Harmonic signals have a crest factor of $Cr = \sqrt{2}$ and time factor of $T_f = 1$ (Pintelon and Schoukens (2012)). They can be expressed by:

$$u(t) = A\cos(2\pi f t + \phi) \tag{18}$$

where A is the amplitude, f the frequency and ϕ is the phase.

Although we can obtain accurate measures with harmonic signals, we are restricted to one frequency at a time. Sweep signals, on the other hand, excite multiple frequencies in a row. They have a crest factor of $Cr \approx 1.45$ and a time factor between 1.5 and 4 (Pintelon and Schoukens (2012)). Sweep signals can be obtained from the following equation:

$$u(t) = A\sin((at+b)t) \qquad 0 \leq t \leq T_0 \tag{19}$$

$$a = \pi(k_2 - k_21)f_0^2, \quad b = 2\pi k_1 f_0, \quad f_1 = k_1 f_0, \quad f_2 = k_2 f_0, \quad f_0 = \frac{1}{T_0}$$

where T_0 is the duration of each sweep loop. The irregular spectrum of sweep signals introduces components with low signal-to-noise ratio and we cannot excite certain frequencies with specific amplitudes. Multisine signals are a general form of harmonic signals that allow us to manipulate the spectrum amplitudes. They are composed of multiple harmonic excitations u_k in the frequencies of interest f_k, $k \in \{1, \ldots, N_f\}$, with phases ϕ_k. Multisine signals can be expressed as in Equation 20:

$$u(t) = \sum_{k=1}^{N_f} u_k = \sum_{k=1}^{N_f} A_k \cos(2\pi f_k t + \phi_k) \tag{20}$$

The choice of amplitudes and phases influences the crest factor. Suitable values can be determined by optimization or iterative methods (see Ojarand and Min (2017), Guillaume *et al.* (1991) and Solomou *et al.* (2002)).

5. RESULTS

In this section, the results obtained with the proposed time-domain methods are compared with Error in Variables (*EIV*) frequency-domain estimator (Pintelon and Schoukens, 2012). The coefficients are compared from 5 Hz to 69 Hz in 4 Hz steps. The Savitzky-Golay filter parameters were chosen in order to avoid attenuation of the frequencies below

100 Hz. The width was set to 71 and polynomial degree to 5. After computing the estimates of velocity and acceleration, the gradient-based and linear regression methods were applied. The optimization algorithm was Adam (Kingma and Ba, 2014), with batch-size of 8192 observations and learning rate of 10^3. Figures 3 and 4 show the estimates for stiffness and damping coefficients, respectively.

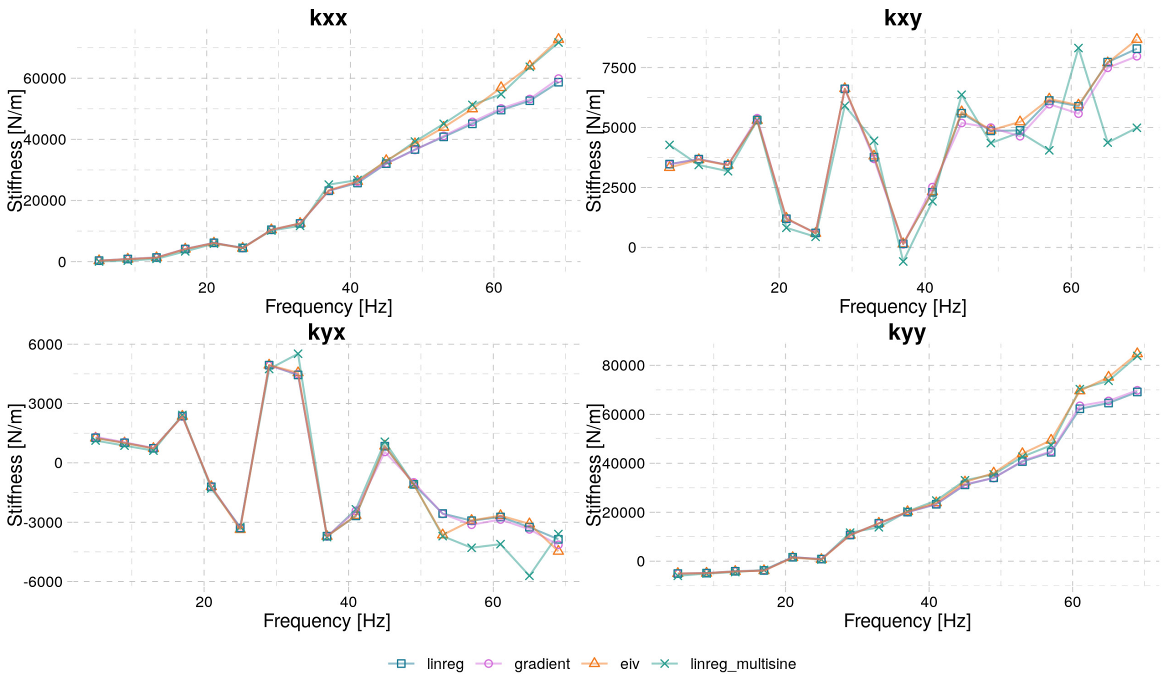

Figure 3: Comparison of estimates of stiffness matrix components for different methods. Frequencies ranging from 5Hz to 69Hz. The EIV is the benchmark frequency-domain method. The EIV, $linreg$ and $gradient$ curves were obtained with harmonic excitation signals; $linreg\_multisine$ multisine excitations.

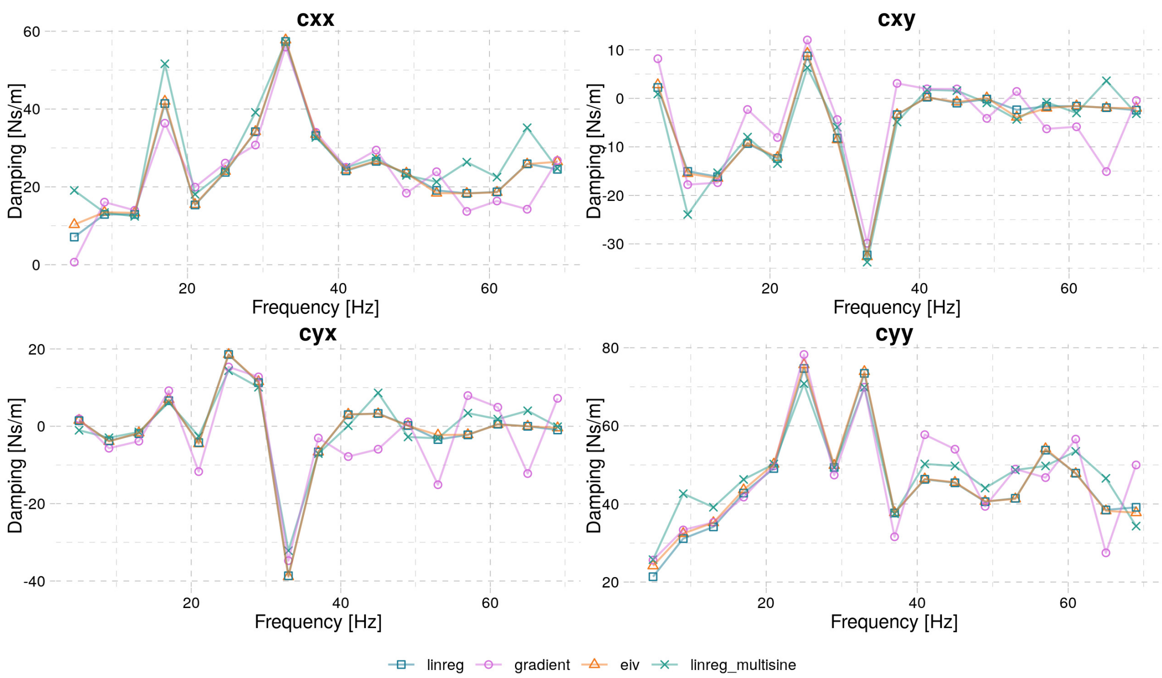

Figure 4: Comparison of estimates of damping matrix components for different methods. Frequencies ranging from 5Hz to 69Hz. The EIV is the benchmark frequency-domain method. The EIV, $linreg$ and $gradient$ curves were obtained with harmonic excitation signals; $linreg\_multisine$ multisine excitations.

The results obtained with linear regression and gradient-based methods using harmonic excitation were similar to the baseline (i.e. the frequency-domain approach) for all coefficients except for direct stiffness components K_{xx} and K_{yy} at higher frequencies, attaining relative error of 18% at 69 Hz. The underestimation of these components might happen due to an attenuation effect of higher frequencies after processing displacement and force measurements with Savitzky-Golay filter. On the other hand, linear regression estimates with multisine excitation presented similar estimated coefficient values in the evaluated band of frequencies, obtaining relative errors of approximately 1% for direct stiffness components. This method also permits faster estimates, since all frequencies are excited simultaneously.

The root mean squared error for stiffness and damping component is summarised in Fig. 5 and Fig. 6. Regarding damping coefficients, linear regression with harmonic signals obtained the smallest errors. The gradient-based method and linear regression with harmonic excitation had similar results for stiffness components, performing better than multisine excitation with respect to cross-coupled stiffness components K_{xy} and K_{yx}.

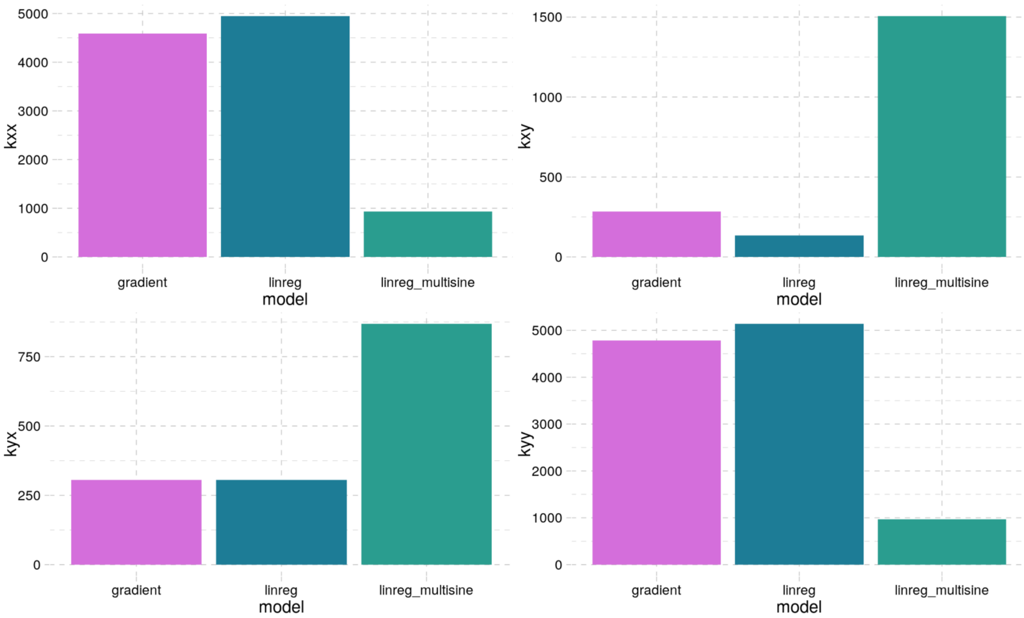

Figure 5: Root mean squared errors of stiffness estimates. Although linear regression with multisine excitation did not perform as good as the other methods for indirect stiffness, it obtained smaller errors for direct stiffness.

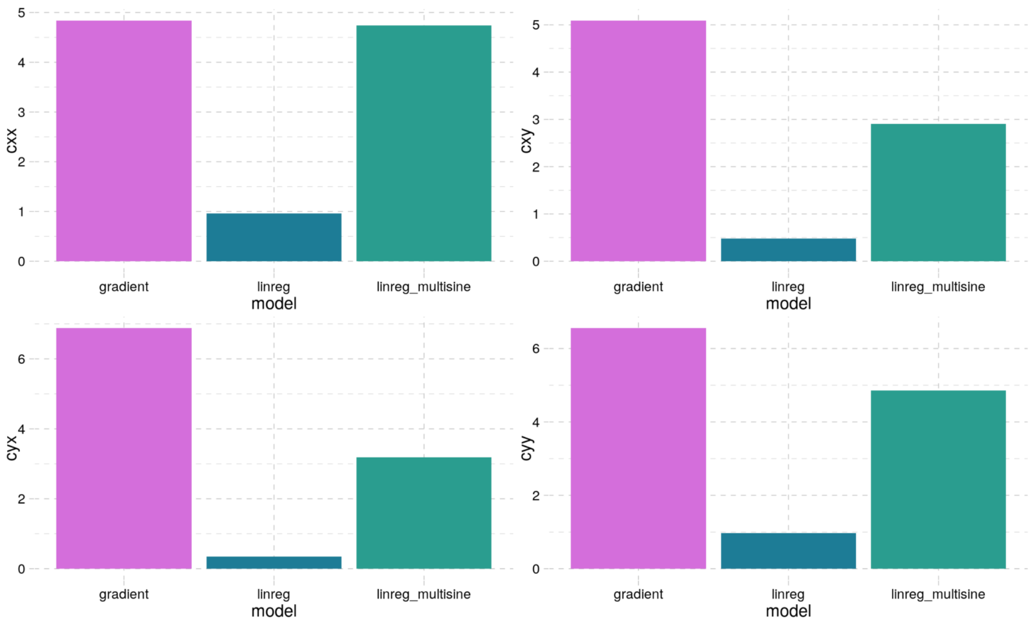

Figure 6: Root Mean squared errors of damping estimates. In terms of quadratic error, Linear regression with harmonic excitation signals acquired the smallest errors.

6. CONCLUSION

In this work, a time-domain approach to system identification applied to active magnetic bearings was proposed. While frequency domain methods depend on acquiring data for multiple periods to increase signal-to-noise ratio, time-domain methods filter the noise in real time. Multiple frequencies can be excited at once and it is not necessary to wait for multiple periods to remove the noise from the data. The projection of multisine signals onto a base of orthogonal harmonic components increases the benefits of using the proposed methods when the experiment duration is an issue.

7. REFERENCES

Brown, T.B., Mann, B., Ryder, N., Subbiah, M., Kaplan, J., Dhariwal, P., Neelakantan, A., Shyam, P., Sastry, G., Askell, A. *et al.*, 2020. “Language models are few-shot learners”. *arXiv preprint arXiv:2005.14165*.

Chasalevris, A., Dohnal, F. and Chatzisavvas, I., 2014. “Experimental detection of additional harmonics due to wear in journal bearings using excitation from a magnetic bearing”. *Tribology International*, Vol. 71, pp. 158–167. ISSN 0301679X. doi:10.1016/j.triboint.2013.12.002. URL `http://dx.doi.org/10.1016/j.triboint.2013.12.002`.

Cranmer, M., Greydanus, S., Hoyer, S., Battaglia, P., Spergel, D. and Ho, S., 2020. “Lagrangian Neural Networks”. pp. 1–9. URL `http://arxiv.org/abs/2003.04630`.

Das, A.S. and Dutt, J.K., 2010. “Control of flexible rotor vibration using electromagnetic actuator based on active disturbance rejection technique”. *Proceedings of ISMA 2010 - International Conference on Noise and Vibration Engineering, including USD 2010*, pp. 1559–1571.

Devlin, J., Chang, M.W., Lee, K. and Toutanova, K., 2018. “Bert: Pre-training of deep bidirectional transformers for language understanding”. *arXiv preprint arXiv:1810.04805*.

Dhariwal, P., Jun, H., Payne, C., Kim, J.W., Radford, A. and Sutskever, I., 2020. “Jukebox: A generative model for music”. *arXiv preprint arXiv:2005.00341*.

Diaz, D.A.G., 2016. “Metodologias De Excitação Para Identificação De Parâmetros Dinâmicos De Selos Anulares”. p. 69.

Donahue, J. and Simonyan, K., 2019. “Large scale adversarial representation learning”. In *Advances in Neural Information Processing Systems*. pp. 10542–10552.

Gorry, P.A., 1990. “General least-squares smoothing and differentiation by the convolution (savitzky-golay) method”. *Analytical Chemistry*, Vol. 62, No. 6, pp. 570–573.

Greydanus, S., Dzamba, M. and Yosinski, J., 2019. “Hamiltonian neural networks”. *Advances in Neural Information Processing Systems*, Vol. 32, pp. 1–16. ISSN 10495258.

Guillaume, P., Schoukens, J., Pintelon, R. and Kollái, I., 1991. “Crest-Factor Minimization Using Nonlinear Chebyshev Approximation Methods”. *IEEE Transactions on Instrumentation and Measurement*, Vol. 40, No. 6, pp. 982–989. ISSN 15579662. doi:10.1109/19.119778.

Hastie, T., Tibshirani, R. and Friedman, J., 2009. *The elements of statistical learning: data mining, inference, and prediction*. Springer Science & Business Media.

Karras, T., Laine, S. and Aila, T., 2019. “A style-based generator architecture for generative adversarial networks”. In *Proceedings of the IEEE conference on computer vision and pattern recognition*. pp. 4401–4410.

Karras, T., Laine, S., Aittala, M., Hellsten, J., Lehtinen, J. and Aila, T., 2020. “Analyzing and improving the image quality of stylegan”. In *Proceedings of the IEEE/CVF Conference on Computer Vision and Pattern Recognition*. pp. 8110–8119.

Kingma, D.P. and Ba, J., 2014. “Adam: A method for stochastic optimization”. *arXiv preprint arXiv:1412.6980*.

Krizhevsky, A., Sutskever, I. and Hinton, G.E., 2012. “Imagenet classification with deep convolutional neural networks”. In *Advances in neural information processing systems*. pp. 1097–1105.

Lillicrap, T.P., Hunt, J.J., Pritzel, A., Heess, N., Erez, T., Tassa, Y., Silver, D. and Wierstra, D., 2015. “Continuous control with deep reinforcement learning”. *arXiv preprint arXiv:1509.02971*.

Mnih, V., Kavukcuoglu, K., Silver, D., Graves, A., Antonoglou, I., Wierstra, D. and Riedmiller, M., 2013. “Playing atari with deep reinforcement learning”. *arXiv preprint arXiv:1312.5602*.

Ojarand, J. and Min, M., 2017. “Recent advances in crest factor minimization of multisine”. *Elektronika ir Elektrotechnika*, Vol. 23, No. 2, pp. 59–62. ISSN 13921215. doi:10.5755/j01.eie.23.2.18001.

Pintelon, R. and Schoukens, J., 2012. *System identification: a frequency domain approach*. John Wiley & Sons.

Robbins, H. and Monro, S., 1951. “A Stochastic Approximation Method”. *The Annals of Mathematical Statistics*, Vol. 22, No. 3, pp. 400–407. ISSN 0003-4851. doi:10.1214/aoms/1177729586.

Savitzky, A. and Golay, M.J., 1964. “Smoothing and differentiation of data by simplified least squares procedures.” *Analytical chemistry*, Vol. 36, No. 8, pp. 1627–1639.

Schulman, J., Wolski, F., Dhariwal, P., Radford, A. and Klimov, O., 2017. “Proximal policy optimization algorithms”. *arXiv preprint arXiv:1707.06347*.

Schweitzer, G. and Maslen, E.H., 2009. “Magnetic bearings. theory, design, and application to rotating machinery”.

Siqueira, R., 2013. “Projeto e implementação de um mancal magnético ativo com controle por modos deslizantes”.

Master's degree, Universidade Federal do Rio de Janeiro, Rio de Janeiro, Brasil.

Solomou, M., Evans, C. and Rees, D., 2002. "Crest factor minimization in the frequency domain". *IEEE Transactions on Instrumentation and Measurement*, Vol. 51, No. 4, pp. 859–865. ISSN 00189456. doi:10.1109/TIM.2002.803510.

Tiwari, R., Lees, A.W. and Friswell, M.I., 2004. "Identification of dynamic bearing parameters: A review". *Shock and Vibration Digest*, Vol. 36, No. 2, pp. 99–124. ISSN 05831024. doi:10.1177/0583102404040173.

Vaswani, A., Shazeer, N., Parmar, N., Uszkoreit, J., Jones, L., Gomez, A.N., Kaiser, Ł. and Polosukhin, I., 2017. "Attention is all you need". In *Advances in neural information processing systems*. pp. 5998–6008.

Zhu, C., Robb, D.A. and Ewins, D.J., 2003. "The dynamics of a cracked rotor with an active magnetic bearing". *Journal of Sound and Vibration*, Vol. 265, No. 3, pp. 469–487. ISSN 0022460X. doi:10.1016/S0022-460X(03)00174-3.

Zou, F., Shen, L., Jie, Z., Zhang, W. and Liu, W., 2019. "A sufficient condition for convergences of adam and rmsprop". *Proceedings of the IEEE Computer Society Conference on Computer Vision and Pattern Recognition*, Vol. 2019-June, No. 1, pp. 11119–11127. ISSN 10636919. doi:10.1109/CVPR.2019.01138.

8. RESPONSIBILITY NOTICE

The authors are solely responsible for the printed material included in this paper.